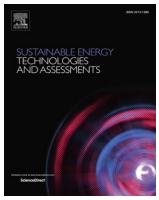
Sustainable Energy Technologies and Assessments 74 (2025) 104187



Contents lists available at ScienceDirect

Sustainable Energy Technologies and Assessments

journal homepage: www.elsevier.com/locate/seta



Review article



Energy harvesting technologies on high-speed railway infrastructure: Review and comparative analysis of the potential and practicality

Wenjing Sun [a,*], David J. Thompson [a], Daniil Yurchenko [a], Dong Zhao [a], Zhenhua Luo [b], Irfan Khan [c]

[a] Institute of Sound and Vibration Research, University of Southampton, Southampton SO17 1BJ, UK
[b] Centre for Energy Engineering, Cranfield University, Cranfield MK43 0AL, UK
[c] HS2 Ltd, Two Snowhill, Snow Hill Queensway, Birmingham, B4 6GA, UK

ARTICLE INFO

Keywords:
Energy harvesting
Railway infrastructure
High-speed rail
Vibration-based harvesting
Wind energy

ABSTRACT

A comprehensive quantitative analysis is provided of the potential applications of energy harvesting (EH) technologies tailored to high-speed railway infrastructure. The study compares the various energy sources within railway infrastructure and identifies suitable EH technologies. Feasible designs and scales of EH are assessed based on the installation location; the overall power availability and energy yield are compared for a notional high-speed railway. For resonant EH devices an assessment is also given of the optimal tuning frequency. Vibration-based EH, when applied to the track or bridge structures, can provide sufficient power for individual low-power sensors; however, its output is insufficient for higher-power applications or for data transmission unless energy storage devices are incorporated. Despite the elevated noise levels generated by high-speed trains, the energy available from this acoustic source is negligible and impractical for EH. Small vertical axis wind turbines installed close to the track and driven by passing trains show great potential, capable of harvesting several orders of magnitude more energy than vibration-based EH. Solar photovoltaic panels can generate significantly more energy than other methods, although their output is confined to daylight conditions and is contingent upon weather conditions.

Introduction

In recent years, there has been considerable interest in energy harvesting (EH) technologies that can power stand-alone equipment without relying on batteries or fixed electrical connections. EH can be utilised for structural health monitoring equipment, sensor networks and other electronic equipment. Railway infrastructure provides a wide range of opportunities for the application of EH to support monitoring equipment. The primary source of energy in this case is the passing train, which generates vibration, sound and wind.

There have been several recent reviews discussing EH applications in railways. Duarte and Ferreira [1] reviewed EH applications on the track, including piezoelectric, hydraulic and electro-mechanical technologies. Subsequently, Hosseinkhani et al. [2] reviewed EH applications on tracks, bridges and vehicles, with emphasis on nonlinear techniques. They also considered the harvesting of sound energy. Bosso et al. [3] and Qi et al. [4] reviewed EH systems installed both on vehicles and on the track. Various EH applications in railways were also reviewed by Zuo et al. [5]. Although these reviews attempt to compare the outputs of different devices, the literature often expresses them in terms of different quantities, such as average power, maximum power, energy per train passage, maximum voltage or current. Moreover, significant differences in train speeds, lengths, and track designs across the studies make it challenging to draw definitive conclusions from simple comparisons. In addition, very few devices have been tested in an operational railway environment and many studies are theoretical or based on laboratory experiments. To relate them to field conditions, estimates of the efficiency of the EH systems are required.

This paper distinguishes itself from previous reviews by providing a systematic critical comparison of EH technologies applied to railway infrastructure. This comparison is based, where possible, on specific examples of practical application taken from the literature. It is supported by a novel classification framework and a quantitative normalisation approach, to enable a like-for-like comparison of EH performance under varying conditions.

The next section explores vibration-based EH from the track, ground

* Corresponding author.
E-mail address: w.sun@soton.ac.uk (W. Sun).

https://doi.org/10.1016/j.seta.2025.104187
Received 18 September 2024; Received in revised form 21 December 2024; Accepted 9 January 2025
Available online 20 January 2025
2213-1388/© 2025 The Authors. Published by Elsevier Ltd. This is an open access article under the CC BY license (http://creativecommons.org/licenses/by/4.0/).

and bridges. As well as summarising published results, a new analysis is provided on the potential of resonant devices, considering the relation between their natural frequency and the vibration spectrum of the track. In the subsequent sections EH from wind induced by train motion and EH from sound are considered. Each section includes a review of relevant literature, with emphasis on applications to operational railways where available. A summary is then given of the power available from the different EH applications for a typical high-speed line with trains of length 400 m running at 320 km/h and compared with solar energy.

Vibration energy harvesting

Suitable vibration-based EH technologies

Electrical energy can be obtained from vibration using piezoelectric (PE), electromagnetic (EM), triboelectric (TE) or electrostatic (ES) transduction mechanisms. PE and EM have been widely investigated and understood, whereas TE and ES are still in their developmental stages and will not be discussed further. PE materials have been utilised in both resonant harvesting devices, which are tuned to a particular excitation frequency, and non-resonant systems, which operate in a broader frequency range. In the following these technologies are discussed separately. The results from these studies will be used to identify typical outputs for the different technologies.

Fig. 1 gives a summary of different technologies that have been applied to vibration EH on railway infrastructure, which will be discussed in more detail below.

Resonant piezoelectric EH

The piezoelectric effect has been well-studied and is considered a relatively simple and cost-effective approach to harvest energy [6]. This section focuses on resonant PE systems; non-resonant systems are covered in the next section. The output from a resonant device is influenced by the relation between its natural frequency and the excitation provided by the passing train. These aspects are discussed in more detail in the section 'Theoretical estimates for resonant vibration-based

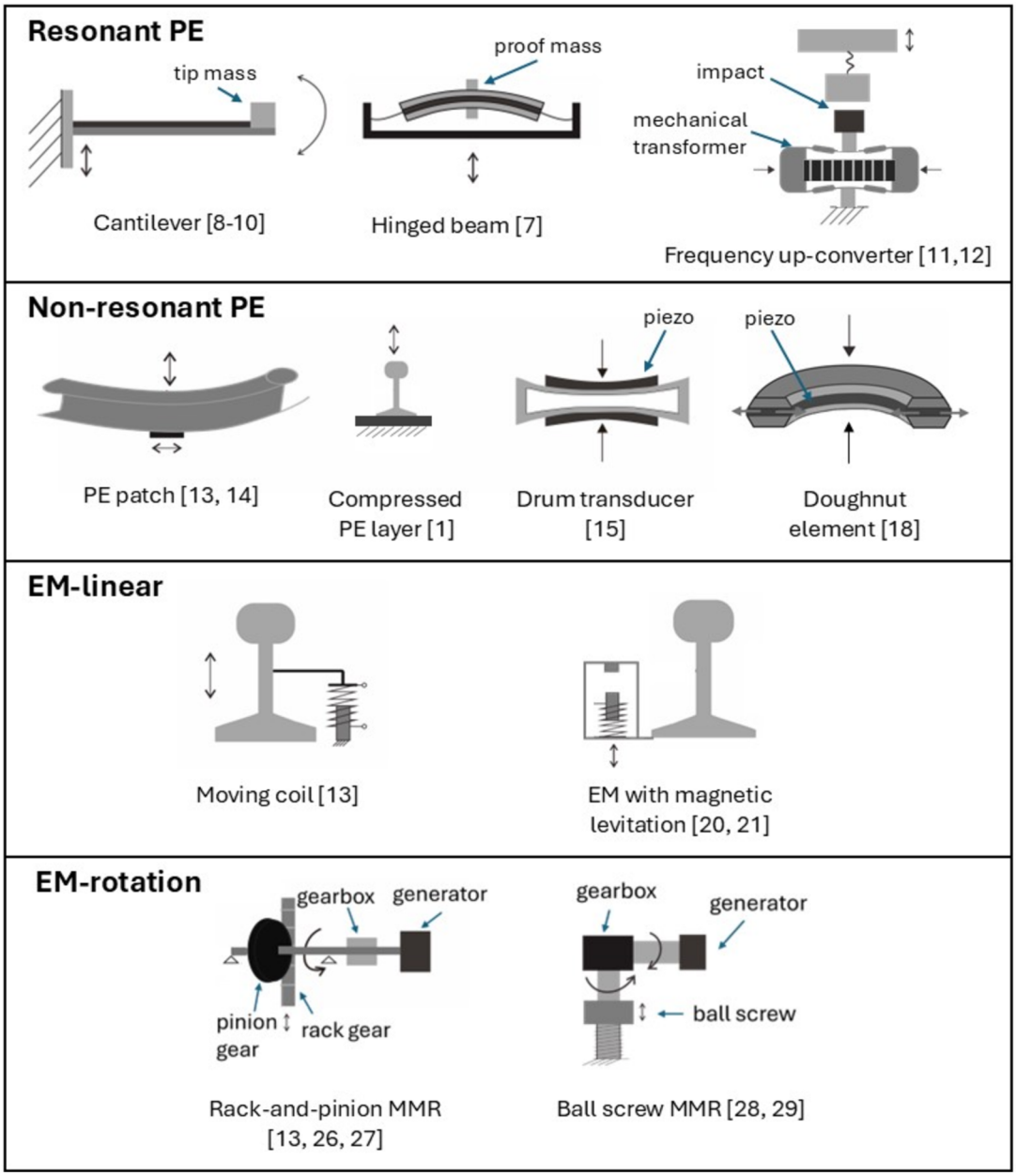


Fig. 1. Illustrative diagrams of vibration energy harvesting devices.

EH' below.

Wischke et al. [7] measured vibration in a railway tunnel in Switzerland, with 'booted' concrete sleepers, resiliently mounted in the base slab. The vibration amplitude of the tunnel wall was too small for effective vibration harvesting, whereas the vibration of the sleepers was found to be suitable. They designed a PE harvester, which consisted of a bimorph beam (i.e. with piezo material on either side of a base structure) supported at each end by solid-state hinges, with a proof mass in the middle. A harvester unit of dimensions 41 mm × 36 mm × 11 mm was designed, with a target frequency range of 380–500 Hz. This contained four parallel beams, tuned to frequencies in this range by using different proof masses, approximately 0.0015 kg each (i.e. combined active mass 0.006 kg). Field tests with the unit installed on a sleeper gave an average energy per train of 395 μJ. It is assumed that the traffic was dominated by long freight trains, travelling at typical speeds of around 100 km/h.

Gao et al. [8] proposed a rail-mounted harvester that consisted of a cantilever of Lead Zirconate Titanate (PZT) with a tip mass of 0.06 kg at one end and the other end clamped to a block attached to the rail. The natural frequency was 23 Hz. Laboratory tests were performed in which a track segment was excited at 5 ~ 7 Hz (intended to be representative of a passenger train with speed 250 km/h). The excitation resulted in a rail displacement amplitude of 0.2 ~ 0.4 mm; a power of 4.9 mW could be obtained.

Li et al. [9] developed an array of six bimorph cantilever beams with natural frequencies 55 ~ 77 Hz, which were mounted on the side of the rail using a block. The proof masses were 0.0035 ~ 0.0041 kg. It was tested on a track traversed by a rail inspection vehicle running at 4 km/h. Due to the very low train speed, the maximum power generated in the field tests was very limited (0.16 μW).

A 3D printed PE EH device was used to collect energy from the vibration of a bridge on a high-speed line in Spain [10]. The device consisted of a bimorph cantilever beam with a tip mass of 0.121 kg and natural frequency of 5.7 Hz, which was tuned to the bridge fundamental mode. It was located on the bridge deck between the two tracks. From 20 train passages, the device generated an average energy of 5.5 mJ per train. The trains, travelling at 230 ~ 290 km/h, were mostly 200 m long.

Shan et al. [11,12] developed piezo-stack EH for application on the rail. A resonant mass-spring system was included with a mass of 0.3 kg and a natural frequency of 18 Hz. A "frequency up-conversion mechanism" was implemented in which the EH system undergoes free vibration at a higher frequency after an initial impact by the mass. The force applied to the piezo stack is amplified by a mechanical transformer. An average power of 7.3 mW was achieved in laboratory tests under a measured track vibration signal corresponding to a train speed of 32 km/h.

Non-resonant piezoelectric EH

In addition to resonant EH systems, a wide variety of non-resonant designs have been proposed using PE materials.

Pourghodrat et al. [13] attached a PE patch to the bottom of a rail, harvesting energy from the longitudinal strain of the rail foot under bending. The size of the patch was not specified. From field tests, an average power of 53 μW was obtained during the passage of an unloaded freight train at 24 km/h. By scaling this, the authors estimated an average power output of 1.1 mW could be expected for a loaded train.

Cahill et al. [14] developed three-dimensional finite element models of energy harvesters, consisting of PE patches bonded to the deck of a railway bridge. Their numerical simulations for the passages of various types of train showed that the power output was largely independent of the train speed, with an average of approximately 370 μW for a passage of a high-speed train with a length of 357 m. This takes 8 s to pass at 160 km/h, resulting in an energy output of 3 mJ per train. Assuming that the power also remains constant at higher speeds, the energy output per train at 320 km/h, with a passage time of 4 s, would be 1.5 mJ. However, this study did not account for the efficiency of the EH system.

Built-in piezo layers or stacks can also be installed under the sleepers or the rail pads to operate in compression; these were described in [1] but no results were presented. Yuan et al. [15] investigated a PE drum transducer placed beneath the sleepers in a ballasted track. Through simulations and reduced-scale laboratory experiments, they showed it could generate up to 100 mW at a train speed of 60 km/h. The energy harvested during the passage of a 6-car metro train was reported to be 400 ~ 500 mJ.

Cao et al. [16] produced a harvester consisting of a stack of circular PE layers in series with a coil spring. This was tested using the theoretical track displacement from an X2 train (length 108 m) travelling at 108 km/h on ballasted track, giving displacements of 1.0 ~ 1.6 mm. The total energy from a train passage was 68 μJ for a duration of about 3.6 s.

Min et al. [17] designed a PE stack harvester mounted between the rail and the slab. Vertical motion of the rail was converted into a transverse force by compression of a shallow top-hat section and used to compress the PE stack. Laboratory tests were performed using sinusoidal inputs.

Min et al. [18] used a stack of doughnut-shaped elements with diameter 100 mm, intended to be located between the rail foot and the slab. Under compression, a ring with a top-hat cross-section applied a radial load to the piezo layers. Laboratory tests were performed with sinusoidal inputs. It was estimated that for a high-speed train of length 200 m running at 230 km/h on a slab track, the output power would be 208 mW. For a 400 m train (duration 6.3 s), the total energy would therefore be 1.3 J.

Electromagnetic induction – Linear harvesters

Electromagnetic (EM) induction is used in EH systems with coils and magnets moving relative to each other. EM harvesters are particularly well suited to low-frequency applications, typically below 100 Hz [19]. In this section, EM harvester systems are considered based on linear (i.e. translational) motion; systems employing rotary motion will be discussed in the following section.

Pourghodrat et al. [13] used a moving coil device to generate electricity from vertical rail deflection. The coil was attached to the rail and moved relative to a fixed magnet. In field measurements, they achieved an average power of 4 mW from an empty freight train running at 18 km/h, and 12 mW from a loaded coal train running at 21 km/h.

Gao et al. [20] proposed an EM-induction harvester. The coil was attached to a plate connected to the rail foot and a magnet was contained within the coil and suspended by magnetic levitation. A field test conducted on a high-speed railway, with trains of length 400 m running on a slab track at 250 km/h, generated an average power of 33.8 mW.

Sun et al. [21] presented an improved design of magnetic-floating EH. From laboratory tests and simulations of application on a rail, they indicated that it could provide an output power of up to around 50 mW. However, no details were given on how to relate the results to a particular train speed or length.

Sun et al. [22] developed an electromagnetic harvester which was mounted on the web of the rail. No details were provided, but this device was combined with a nonlinear PE transducer, which was used to detect rail corrugation. Laboratory tests included inputs based on measured rail vibration, which yielded 18.7 mW under normal rail conditions on a slab track. The train speed was 81 km/h, with a duration of approximately 8.2 s, implying a train length of approximately 185 m. The pass-by energy can be estimated as $8.2 \times 18.7 = 153$ mJ.

Hou et al. [23] proposed a linear EH device for installation between a floating track slab and bridge deck. It consisted of a large block (1500 kg), mounted on helical springs, with two permanent magnets, and electrical coils. Their assessment was based on numerical simulations and indicated an average power of 0.6 W at its natural frequency of 5.5 Hz.

Electromagnetic induction – Rotary energy harvesters

Rotary EM harvesters have been developed by utilizing a mechanical

motion rectifier (MMR) to convert the bidirectional vibration into unidirectional rotation of a shaft, which then drives a generator to produce electricity [4]. None of these MMR systems have been applied to high-speed trains but there are many laboratory studies, which show the mechanical efficiency can be greater than 50 % [24,25].

Pourghodrat et al. [13] developed a rotary EH device based on a rack-and-pinion system. The rack gear was fixed into the subgrade, while the pinion gear moved vertically on it driven by the track motion. The unit was installed across two sleepers in a ballast track. From field tests with a loaded freight train travelling at 18.5 km/h, giving a vertical deflection of 12.7 mm, the average power was 220 mW.

Lin et al. [26] developed an anchorless MMR track EH based on a similar mechanism by incorporating preloaded reset springs that counteract the harvester force during track upward motion. Field testing produced an average power of 6.9 W for a freight train travelling at 64 km/h.

Zhang et al. [27] proposed an EM vibration EH for freight railroads based on a rack-and-pinion design with the rack attached to the rail foot. Laboratory experiments were performed with sinusoidal inputs, and simulations indicated an average power during a freight train passage of 0.55 W at 60 km/h and 1.29 W at 120 km/h.

Pan et al. [28] developed a compact ball-screw based harvester with MMR. In field tests, the harvester was attached to the rail on a ballast track. The best configuration achieved an average power of 2.24 W during operation of a two-car metro vehicle running on a test line at 30 km/h.

Pan et al. [29] also implemented this type of EH device within a railway sleeper. The sleeper was supported on springs inside a box and two harvesters were installed, one under each rail. In laboratory experiments, they reproduced the deflections in a ballasted track during the passage of a freight train at 64 km/h. They reported a power output of up to 45 W from a half sleeper, i.e. up to 90 W for the full width. The vertical displacements were of the order of 4 mm, whereas in a high-speed track they would be much smaller.

Summary and analysis

Table 1 summarises the results presented in this section. Where the literature reports average powers, these have been recalculated here to represent the energy per train passage, based on the given train length and speed; for both freight and high-speed trains a common length of 400 m is assumed.

Focussing first on the applications to high-speed rail, a PE cantilever with a tip mass of 0.06 kg achieved 28 mJ [8]. PE patches, such as in [13], generally produce smaller amounts of energy for equivalent conditions. Based on laboratory experiments, the PE drum transducer of [15] produced 490 mJ during the passage of a six-car metro train at 60 km/h. The circular PE stack of [16] produced only 70 μJ, whereas the stack of doughnut-shaped elements is estimated to produce 1.3 J for a high-speed train at 230 km/h [18].

With linear EM, 190 mJ can be harvested from a high-speed train

Table 1
Summary of results for vibration-based EH from literature.

	Type	Location	Track	Train type	Train speed, km/h	Power, mW	Train length, m	Duration, s	Energy per train, J	Ref	Notes
Resonant PE	Hinged beams, 440–500 Hz	On sleepers	Slab	Mainly freight	100	N/A	N/A	N/A	0.0004	[7]	Train details assumed
	Cantilever beam, 23 Hz	On rail	Slab	High-speed	250	4.9	400	5.76	0.0282	[8]	Based on laboratory tests; energy calculated for 400 m train
	Cantilever beam, 5.7 Hz	On bridge deck	Ballast	High-speed	230–290	N/A	400	N/A	0.011	[10]	Energy extrapolated to train length 400 m
	PE stack with frequency up-conversion	On rail	Ballast	Unknown	32	7.3	N/A	N/A	N/A	[12]	Based on laboratory tests
Non-resonant PE	Adhesive patch	On rail	Ballast	Freight (loaded)	24	1.1	400	60	0.066	[13]	Energy calculated for 400 m train
	Adhesive patch	On bridge	N/A	High-speed	320	0.37	357	4.0	0.0015	[14]	Based on simulations; results extrapolated to 320 km/h
	Drum transducer	Under sleeper	Ballast	Metro	60	100	150	9.0	0.49	[15]	Based on laboratory tests
	Circular PE stack	Under rail	Ballast	High-speed	108	0.019	108	3.6	0.00007	[16]	Based on laboratory tests
	Stack of donut-shaped elements	Under rail	Slab	High-speed	230	208	400	6.3	1.3	[18]	Based on laboratory tests
Translational EM	EM induction	On rail	Ballast	Freight (loaded)	21	12	400	103	0.82	[13]	Energy calculated for 400 m train
	EM induction	On rail	Slab	High-speed	250	33.8	400	5.76	0.19	[20]	
	EM induction	On rail	Slab	Metro	81	18.7	185	8.2	0.33	[22]	Based on laboratory tests
Rotary EM	Rack and pinion MMR system	Across two sleepers	Ballast	Freight (loaded)	18.5	220	400	117	17	[13]	Energy calculated for 400 m train
	Rack and pinion MMR system	Beneath rail foot	Ballast	Freight	120	1,290	400	12	15.5	[27]	Based on lab tests; energy calculated for 400 m train
	Rack and pinion MMR system	Across two sleepers	Ballast	Freight (loaded)	64	6,900	400	34	155	[26]	Energy calculated for 400 m train
	Ball-screw based MMR system	On rail	Ballast	Metro	30	2,200	50	N/A	N/A	[28]	
	Ball-screw based MMR system	Inside sleeper	Ballast	Freight (loaded)	64	90,000	400	34	2,020	[29]	Based on laboratory tests; energy calculated for 400 m train

[20]. However, there are no results available for rotary EM devices applied to high-speed rail. Nevertheless, comparing the various results from [13] for freight trains, MMR can achieve approximately 20 times the energy of linear EM. Although this shows significant potential, it has not yet been demonstrated on a high-speed line, where the track deflections will be much smaller than on the freight lines in [13], and the loading frequencies are higher.

Theoretical estimates for resonant vibration-based EH

In-service vibration amplitudes

For resonant EH systems, the energy harvested depends strongly on the relation between the natural frequency of the device and the excitation provided by the train. In this section, estimates of the vibration of a high-speed track are combined with theoretical calculations of the output from a resonant EH device. This allows the optimal tuning frequencies and the corresponding energy to be determined.

The semi-analytical model for railway ground vibration, MOTIV [30] is used to obtain an estimate of the vibration amplitudes and dominant frequencies of the rail, slab and adjacent ground for a high-speed train running on slab track. The model has been run for a train speed of 320 km/h (89 m/s), with parameters representative of a typical slab track (rail fasteners with dynamic stiffness 50 MN/m) on a moderately soft ground. The train consists of vehicles each 25 m long. Results are obtained for the vibration on the rail, the slab, and the ground at different distances from the track centreline. They are shown as one-third octave acceleration spectra in Fig. 2(a). Corresponding results for a typical ballasted track with rail pad dynamic stiffness of 120 MN/m are shown in Fig. 2(b). The overall RMS acceleration amplitudes deduced from these spectra are listed in Table 2, together with the amplitudes in selected one-third octave bands.

Dominant frequencies

Although it is masked to some extent by the one-third octave band presentation, the frequency content of the track (and ground) vibration at low frequencies is dominated by the so-called trainload frequencies [31]. These are integer multiples of the vehicle passing frequency, $f_n = nv/L$, where v is the train speed (in m/s), L is the vehicle length and n is an integer. Depending on the bogie spacing and wheelbase, different peak frequencies are dominant, but Milne et al. [31] found that for most train geometries, the peaks at $n = 3$ and $n = 7$ are particularly prominent.

For $v = 89$ m/s and a nominal vehicle length $L = 25$ m, as used in Fig. 2, the vehicle passing frequency is 3.6 Hz, while the 3rd and 7th trainload frequencies are 10.7 Hz and 25 Hz. The acceleration levels corresponding to these frequencies can be approximated by extracting the RMS acceleration amplitudes from Fig. 2 in the 4 Hz, 10 Hz and 25 Hz one-third octave bands, as listed in Table 2. The amplitudes at 4 Hz are typically 1–2 orders of magnitude smaller than those at 25 Hz.

Table 2
RMS acceleration amplitudes (m/s^2) during passage of a high-speed train, calculated from Fig. 2.

Track type	Position	Total	4 Hz	10 Hz	25 Hz	80 Hz
Slab track	Rail	7.2	0.13	0.86	1.65	3.7
	Slab	1.2	0.076	0.41	0.13	0.65
	Ground, 2 *m*	0.48	0.036	0.19	0.079	0.24
	Ground, 4 *m*	0.26	0.004	0.021	0.053	0.10
Ballast track	Rail	6.5	0.111	0.937	2.30	2.09
	Sleeper	5.1	0.088	0.747	1.86	1.57
	Ground, 2 *m*	1.4	0.035	0.300	0.621	0.429
	Ground, 4 *m*	0.39	0.0038	0.033	0.087	0.153

Fig. 2 also shows a peak at 80 Hz, corresponding to the resonance of the unsprung mass of the axles on the overall stiffness of the track, known as the P2 resonance. This peak is more prominent for the slab track than for the ballasted track. The RMS acceleration in the 80 Hz frequency band is also listed in Table 2.

Another excitation frequency of importance is the sleeper-passing frequency. However, for a train speed of 320 km/h and a sleeper/fastener spacing of 0.6 m, this occurs at about 150 Hz, which is outside the range considered here. For a train speed of 160 km/h, it would occur at about 75 Hz, aligning more closely with the P2 resonance and leading to a more prominent peak in the vibration spectrum.

Bridge vibration

For EH from bridge vibration, spectral peaks also occur at the natural frequencies of the bridge span. Especially high amplitudes can be expected if one of the trainload frequencies coincides with the bridge fundamental frequency, although this should normally be avoided by design. Bridges with a span of 60 m have a natural frequency of 2 ∼ 4.5 Hz, while a 30 m span bridge has a natural frequency of 4 ∼ 9 Hz [32].

Galvin et al. [33] recently measured the vertical acceleration on a concrete bridge on a high-speed line in Spain. The bridge spans were 24 m and their fundamental bending mode was estimated as 6.3 Hz. This was therefore the target frequency of the EH study in [10].

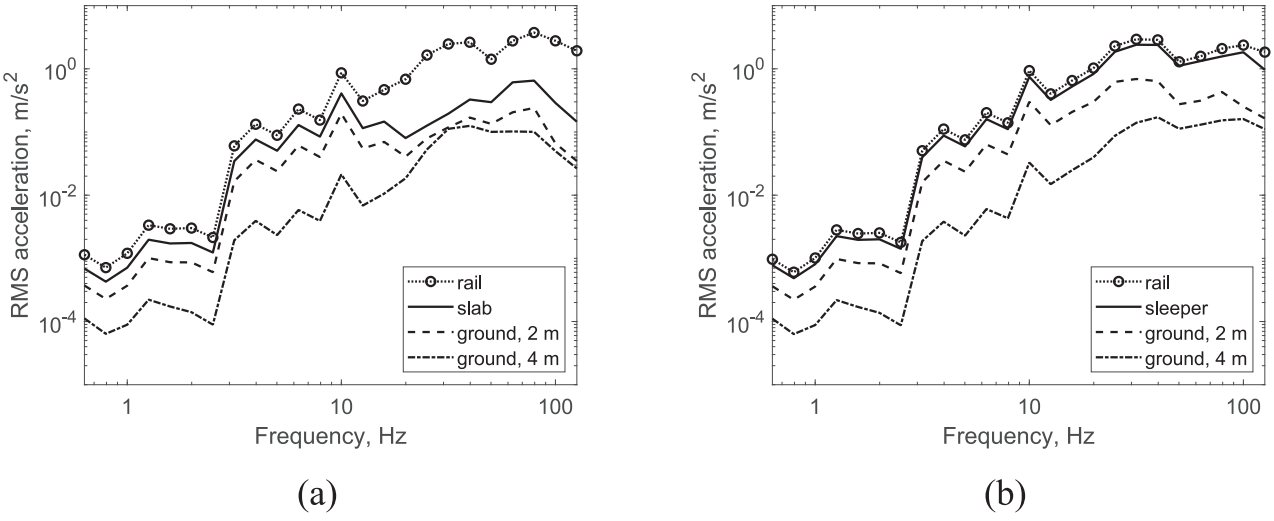


Fig. 2. One-third octave spectra of vibration from a high-speed train at 320 km/h running on (a) a slab track and (b) a ballasted track, predicted using the MOTIV model.

Application to resonant vibration EH

As noted in the previous section, vibration-based EH devices are often based on a resonant system. Gatti et al. [34] presented a theoretical study of a generic EH device attached to the track, and investigated the optimum parameters including the tuning frequency of the device. Simulations were performed using accelerations measured on a sleeper of a ballasted track during the passage of a train of length 200 m running at 195 km/h (54 m/s). The maximum energy that could be harvested per unit active mass of the device was found to be approximately 0.25 J/kg at a frequency of 17 Hz, which corresponded to the 7th trainload frequency. This was based on an optimal damping ratio of 0.0045.

For a passing train, the device takes some time to reach steady-state conditions, and for a lightly damped system the time is longer. However, for parameters typical of a high-speed train and damping ratios of 0.01 or greater, it is the steady-state conditions that determine the energy harvested. In this case, the total energy harvested is approximately [34]

$$E(t_e) \approx \frac{\ddot{Y}^2 m}{4\zeta\omega_n} t_e \tag{1}$$

where $\ddot{Y}$ is the base acceleration amplitude, m is the active mass of the harvester, ω_n is the circular natural frequency assumed equal to the excitation frequency, ζ is the damping ratio and $t_e = L/v$ is the duration of the excitation signal, where L is the train length and v is its speed. This formula gives the maximum theoretical energy, assuming that all dissipated energy can be recovered, whereas in practice there are other sources of damping present. Therefore, allowance should also be made for the efficiency of generation.

Table 3 lists the energy per train passage, calculated from equation (1) at different frequencies and positions using the RMS acceleration amplitudes from Table 2 for the examples of the slab track and ballast track. These values are per train passage and normalised by the active mass; for PE EH devices this is typically 0.001 ∼ 0.1 kg [10,35]. On the slab, or on the ground at 2 m from the track centre, the highest energy is obtained at 10 Hz, whereas on the rail or further from the track the energy is highest at 80 Hz. For the ballasted track, the highest energy is obtained at 25 Hz at each location.

From these results, for applications on slab track it appears to be more beneficial to tune an EH device to the P2 resonance, as also found by Hussein et al. [36], or to the 3rd trainload frequency (10 Hz). For a ballasted track, where the P2 resonance is less prominent, the best results are obtained by tuning the harvester to the 7th trainload frequency (25 Hz), as found by Gatti et al. [34].

To apply these theoretical results, it is necessary to account for the efficiency of the device. Cámara-Molina et al. [37] found that the energy harvested from a resonant PE device attached to a bridge varied greatly between different train passages. This variation is due to differences in train speed and axle spacing, because of which the excitation frequencies do not always match the tuning frequency of the device. Consequently, only 2 or 3 out of the 18 train passages contributed significantly to the overall energy harvested for a given tuning frequency.

To give a realistic estimate of the potential for resonant PE devices to harvest energy from train passages, it is assumed therefore that the energy harvested is limited to 10 % of the ideal calculation. Moreover, assuming an efficiency of 50 % for the device itself, the overall estimate is taken as 5 % of the ideal calculation listed in Table 3. This factor will be used in the comparisons below.

Table 3
Energy per train passage from resonant EH system, train speed 320 km/h, train length 400 m, damping ratio 0.01 expressed per kg of active mass.

Track type	Position	At 4 Hz (J/kg/train)	At 10 Hz (J/kg/train)	At 25 Hz (J/kg/train)	At 80 Hz (J/kg/train)
Slab track	Rail	0.16	2.7	3.9	6.3
	Slab	0.052	0.60	0.023	0.19
	Ground, 2 m	0.012	0.14	0.009	0.026
	Ground, 4 m	0.0001	0.0016	0.0040	0.0045
Ballast track	Rail	0.11	3.1	7.5	2.0
	Sleeper	0.069	2.0	5.0	1.1
	Ground, 2 m	0.011	0.32	0.55	0.08
	Ground, 4 m	0.0001	0.0039	0.011	0.011

Wind energy harvesting

This section considers harvesting energy from the air flow generated by the train movement by using small wind turbines located close to the track.

Wind EH technologies

There are three main types of wind turbine used to harvest energy: horizontal axis wind turbines (HAWT) and vertical axis wind turbines (VAWT), which may be divided into Savonius and Darrieus designs, see Fig. 3. The theoretical power available in an air flow can be calculated from

$$P = \frac{1}{2}\rho u^3 A \tag{2}$$

where $\rho = 1.2\text{kg/m}^3$ is the density of air, u is the flow speed and A is the cross-section area. The power output from a wind turbine is therefore $P_{\text{out}} = \eta P$, where η is its efficiency. For a HAWT, the area $A = \pi R^2$, where R is the radius of the turbine, while for a VAWT, $A = DH$, where D is the diameter and H is the height of the working part of the turbine.

VAWTs have a number of benefits; compared with HAWTs they occupy less space, are less expensive, and have a lower minimum operating speed. However, the efficiency of VAWTs tends to be lower than that of large HAWTs, which can reach over 40 % [38].

Comparing the two main types of VAWT, the Darrieus design usually requires an additional power source to start the turbine rotation [39], making it less feasible for applications where both the wind speed and duration are low. The Savonius rotor requires a lower cut-in wind speed and also has advantages of simplicity, reliability and low noise levels [40]. The efficiency of the Savonius rotor (maximum around 15 %) is usually lower than that of the Darrieus one (up to 40 %), although the efficiency could be improved by a hybrid design, which integrates both types of rotor [41]. An example of a Savonius VAWT located close to moving trains is given by Sekhar et al. [42], while Tairab et al. [43] developed a combined harvester consisting of a small Savonius wind turbine and a solar panel for implementation along railway lines.

Open route train-induced wind EH

There is potential for installing small wind turbines close to the track to harvest energy from the aerodynamic flow and turbulence generated around high-speed trains. On open route these disturbances largely die out within around 3 m from the track. To assess their energy output, information about the flow speed at different lateral positions is utilised from measurements in [44,45]. The velocity profile generated by passenger and freight trains was presented at various distances from the track. Some approximate results are summarised in Table 4, which are based on the average measured results for an ICE1 train, at a mean height of 0.5 m above the rail head, with the flow speed u shown normalised by the train speed v. These are then used to determine the approximate average flow speed for a train speed of 320 km/h and the corresponding power in the air flow, calculated from equation (2).

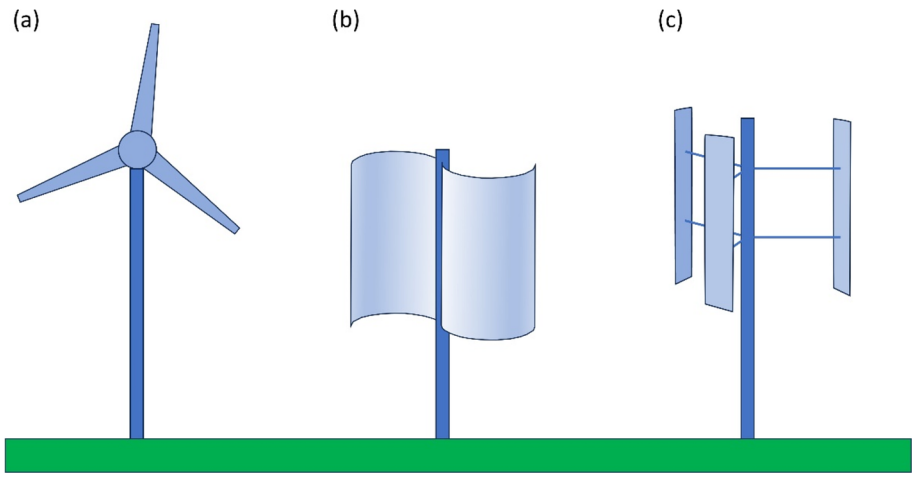


Fig. 3. The three main types of wind turbine: (a) HAWT, (b) Savonius VAWT, and (c) Darrieus VAWT.

Table 4
Average flow speed u and maximum available power at distance y away from the track centre and a height of 0.5 m above the rail head (open route) as well as power and energy per train from a VAWT of 0.25 × 0.25 m during a train passage at 320 km/h (89 m/s).

y, m (from track centre)	Normalised flow speed u/v	Flow speed u, m/s	Power in flow per unit area, W/m^2	Output power from VAWT, W	Energy per train from VAWT, J
1.91	0.225	20	4800	45	203
2.25	0.135	12	1040	9.7	44
2.85	0.065	5.8	117	1.1	4.9
3.17	0.055	4.9	71	0.66	3.0

These results are used to calculate the power and energy that would be harvested by a wind turbine during a single train passage for a train length of 400 m and a speed of 320 km/h. The power and energy values listed in Table 4 are derived from the above equations, assuming an efficiency of 15 % for a VAWT with a nominal cross-section of 0.25 × 0.25 m. Note that these calculations do not account for the energy harvested from ambient wind, which would also contribute to the overall energy yield [42].

A VAWT can be tuned for a specific train speed and surrounding conditions, by changing the ratio of its height (H) to diameter (D). The smaller this ratio, the higher the efficiency of the VAWT for a given frontal area [46].

Train-induced wind EH in tunnels

A similar concept can be used in tunnels to harvest wind energy, where, depending on the tunnel design, it is possible to install small wind turbines on the inner wall of the tunnel. For a typical high-speed tunnel design, this could allow for the installation of a VAWT with an area of up to 1 m^2. However, for consistency with the open route deployment, dimensions of $H = 0.25$ m and $D = 0.25$ m are assumed.

Airflow patterns in tunnels differ from open route since the tunnel restricts the sideways wind propagation, pushing it forward and balancing the built-up pressure through ventilation ducts. The flow speeds are roughly constant across the tunnel cross-section, so they no longer depend on the distance from the train. Examples of calculated flow speeds in a tunnel are given in [45] for a train speed of 200 km/h (55 m/s). These were calculated for a position 500 m into a tunnel of length 2000 m. For most of the time that the train is in the tunnel, the air is pushed ahead of the train or pulled behind it, but as the train passes the observation point the flow is backwards towards the entrance. Approximate values for the flow speeds presented in [45] are expressed as a percentage of the train speed in Table 5. The flow speeds are then recalculated for a train speed of 320 km/h (89 m/s). The theoretical power available from this air flow can be calculated from equation (2). The power that can be generated by each wind turbine is also listed in Table 5, assuming a VAWT with efficiency 15 %.

The duration of this power generation depends on the length of the tunnel, the location of the wind turbine within the length of the tunnel and the train speed. For example, taking the length of the tunnel (or the distance between two ventilation shafts) as 3 km, and considering a high-speed train length of 400 m, the train will pass through this section of tunnel in 38.2 s. If power is only generated during this time, for a VAWT located at the centre of this section of tunnel, the energy produced by one train passage would be around 145 J, as indicated in Table 5. The average power is given by dividing this energy by the total transit time. An assessment of the output from multiple VAWTs in a tunnel is given later. To select an appropriate VAWT, the design would need to be matched to the expected wind speeds.

Acoustic energy harvesting

Acoustic energy has been proposed as a potential source for energy harvesting by several researchers, e.g. [47,48]. To estimate the energy available from the noise generated by a high-speed train, Fig. 4(a) shows one-third octave noise spectra measured during the passage of TGV trains, at 25 m from the track [49].

The total unweighted sound pressure level (SPL) L_p can be calculated from these results, using the formula [50]

Table 5
Estimates of flow speed induced by a train in a tunnel and available power as well as power and energy per train from a VAWT of 0.25 × 0.25 m during a train passage at 320 km/h (89 m/s).

	Flow speed relative to train speed, u/v	Flow speed u, m/s	Power in flow per unit area, W/m^2	Output power from VAWT, W	Pass-by time, s	Energy per train from single VAWT, J
Ahead of train	4 %	3.2 m/s	20	0.19	16.85	3.2
During the train passage	−15 %	−13 m/s	1300	12.2	4.5	54.9
After train passage	11 %	10 m/s	550	5.15	16.85	86.7
Total				3.79	38.2	144.9

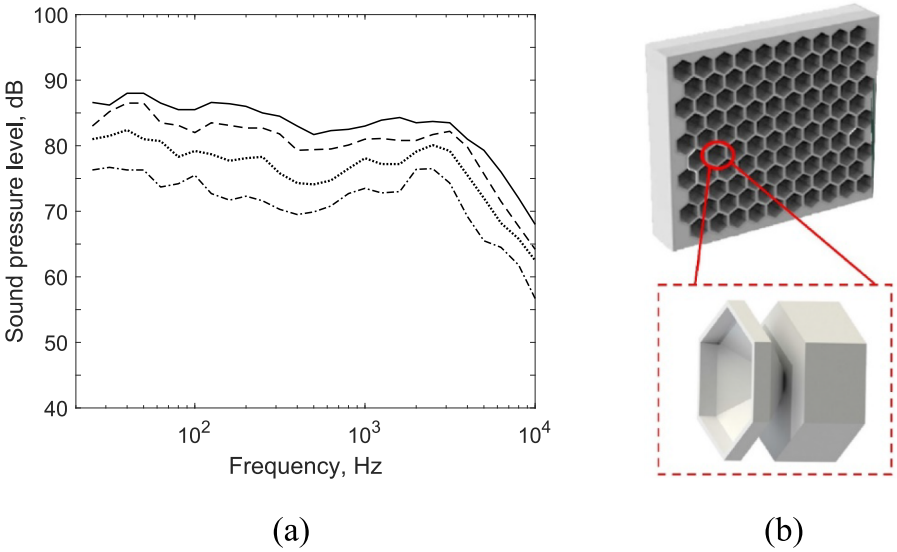


Fig. 4. (a) Typical one-third octave noise spectra at 25 m from a TGV-Duplex train running at different speeds; – · – · 200 km/h; ····· 250 km/h; – – – 300 km/h; — 350 km/h [49]. (b) Acoustic EH device proposed by Wang et al. [47].

$$L_p = 10\log_{10}\left(\sum_{i=1}^{N} 10^{\left(\frac{L_{p,i}}{10}\right)}\right) \tag{3}$$

where $L_{p,i}$ is the SPL in dB in frequency band i and there are N frequency bands.

Interpolation of these results yields a SPL of 97.3 dB at 320 km/h. Assuming that the train can be represented as a line source, the SPL at different distances from the source x can be determined using [50]:

$$L_p(x) = L_p(x_0) - 10\log_{10}\left(\frac{x}{x_0}\right) \tag{4}$$

Hence, the SPL can be converted from the value at $x_0 = 25$m to give the value at $x = 5$m as 104.3 dB. The sound intensity level in dB re 10^{-12} W/m^2 is approximately equal to the SPL in dB re 2×10^{-5} Pa [50], so the overall sound intensity at 5 m is:

$$I = 10^{\left(\frac{L_p}{10}\right)} \times I_{\text{ref}} \tag{5}$$

where $I_{\text{ref}} = 10^{-12}$ W/m^2 is the reference value used for sound intensity; in this case this gives $I = 10^{10.43} \times 10^{-12} = 0.027$W/m^2

From these estimates, it can be concluded that the amount of energy available in the acoustic field is small. Moreover, the existing acoustic EH devices that can capture this energy generally have a low efficiency. For example, Wang et al. [47] reported a harvested power of 0.59 μW for a SPL of 100 dB using a Helmholtz resonator-based unit, shown in Fig. 4 (b). The unit had an approximate area of 0.01 m^2, so this corresponds to a power density of 59 μW/m^2. It is necessary to allow for the bandwidth of the acoustic signal in the tests in [47], which covered the range 270–600 Hz (about 3.5 one-third octave bands), whereas the device was effective only within a single one-third octave band. The equivalent SPL in a single band would be $100 - 10\log_{10}(3.5) = 94.5$ dB, corresponding to an incident sound intensity (from equation (5)) of 2.8 mW/m^2. Comparing this with the harvested power of 59 μW/m^2, the efficiency can be estimated as 2 %.

To estimate the power that can be harvested from a passing high-speed train, this efficiency should be applied to one-third octave band sound intensities. The average one-third octave band sound level (over 25 ~ 2000 Hz) obtained from the results in Fig. 4(a), and converted to a distance of 5 m (using equation (4)), is 90 dB, which corresponds to 1.0 mW/m^2. Applying the efficiency of 2 % to this value gives the harvested power as 20 μW/m^2. The potential for using such systems in noise barriers is discussed in Section 5 below.

Comparison of EH technologies

Summary of available power

To allow direct comparisons between different EH technologies, the power that could be harvested from various energy sources is summarised in this section. To provide a common basis, a high-speed train with length 400 m running at 320 km/h is assumed. To arrive at quantitative comparisons some rather coarse assumptions are necessary, so the results should be considered as order-of-magnitude estimates.

Comparisons are given first in Table 6 in terms of the power from a single EH unit. Suitable designs and parameters of EH devices are selected for each technology, as follows:

(1) For vibration-based EH using resonant PE devices, calculations are based on the energy E' per train per unit mass, given in Section 2.2 (Table 3). An active mass of $m = 0.05$kg is assumed and an overall efficiency of $\eta = 0.05$ is applied to these theoretical estimates. The pass-by time for a train of length 400 m and speed 320 km/h is $T = 4.5$s. Hence, the power listed in Table 6 is obtained as $W = E'm\eta/T$. At each location the natural frequency is chosen to give the highest power. These results for application on the rail are found to be broadly consistent with those reported in Table 1 for resonant PE (if they are normalised by the active mass).
(2) For application of resonant PE devices on a bridge, the values from [10] are included, which were measured on a ballasted track.
(3) The results for non-resonant PE and for EM vibration-based devices are derived from the power given in Table 1. They are converted to correspond to an overall rail deflection of 0.4 mm, assuming that the power is proportional to the square of the deflection amplitude Δx. The assumed deflections are also listed in Table 6. However, no correction has been made here for train speed.
(4) According to the average wind speeds due to train passages, presented in Table 4 for different distances from the track, the power from small VAWTs in the open route is determined assuming a blade diameter 0.25 m, height 0.25 m and efficiency of 15 %.

Table 6
Comparison of the power harvested by different EH technologies applied to high-speed infrastructure.

Energy source	Position (distance from track centre)	Natural frequency, Hz	Deflection Δx, mm (if used)	EH unit	Power, W
Vibration, resonant PE (Slab track)	Rail	80	–	0.05 kg	3.5×10^{-3}
	Slab	10	–	0.05 kg	3.3×10^{-4}
	Ground, 2 m	10	–	0.05 kg	7.8×10^{-5}
Vibration, resonant PE (Ballast track)	Rail	25	–	0.05 kg	4.2×10^{-3}
	Sleeper	25	–	0.05 kg	2.8×10^{-3}
	Ground, 2 m	25	–	0.05 kg	3.1×10^{-4}
Vibration, resonant PE	Bridge	6.7	–	0.121 kg	2.0×10^{-3}
Vibration, non-resonant	Rail	–	12.7	PE patch	1.1×10^{-6}
	Rail	–	12.7	EM induction	1.2×10^{-5}
	Sleeper	–	6.0	Rack and pinion	3.1×10^{-2}
	Sleeper	–	4.0	Ball screw MMR	0.9
Wind (VAWT)	1.91 m	–	–	0.25×0.25 m^2	45
	2.25 m	–	–	0.25×0.25 m^2	9.7
	2.85 m	–	–	0.25×0.25 m^2	1.1
	3.17 m	–	–	0.25×0.25 m^2	0.7
	Tunnel	–	–	0.25×0.25 m^2	3.8
Sound	5 m	–	–	per m^2	2.0×10^{-5}

(5) In tunnels, the same dimensions of VAWT are assumed for consistency. The power harvested is greater behind the train than in front (see Table 5), so the energy output will vary depending on the turbine position along the length of the tunnel. Nevertheless, the average over multiple wind turbines will be approximately equal to the value from the centre of the tunnel, given in Table 5, used here.
(6) The power efficiency of the acoustic EH devices attached to noise barriers is assumed to be 2 %, based on the sound within a single one-third octave band, as discussed in Section 4.

It should be noted that the size of the EH devices varies considerably between the different technologies. Although it would be possible to normalise by the volume or mass, this is not attempted here due to sparsity of detailed information.

The main purpose of EH is to provide power for remotely operating sensors or a sensor network and data transmission unit. The power requirements can vary depending on the type of sensor and the frequency of measurements, typically in the range 0.1 ~ 100 mW [4]. Data transmission units, depending on the transmission distance and frequency, may consume up to several watts.

According to the values listed in Table 6, the power from acoustic EH with an area of 1 m^2 is not sufficient to meet the smallest of these values; the same is true for vibration-based EH on the ground or from a PE patch on the rail or EM induction on the rail. The ball screw MMR system in the sleeper and all VAWT applications meet the full range of requirements for sensors and may even provide sufficient power to allow data transmission. The other vibration-based EH devices provide power within the range of the required values. In cases where EH does not meet the power requirements for data transmission, an energy storage device would be necessary to provide a higher power over a short time interval. A review of energy storage systems is given in [51].

Summary of available energy for typical installation

To enable direct comparisons between different EH technologies, the amount of energy that can be harvested from various sources is summarised in this section, based on the information presented in previous sections. The results are listed in Table 7.

Results are presented first of the energy per train pass-by from a single EH unit. In most cases these values are obtained from the power listed in Table 6 multiplied by the pass-by duration of 4.5 s. The energy in joule is divided by 3600 to give the result in Wh. However, for the non-resonant vibration-based EH, the results are from lower speed trains so the pass-by durations from Table 1 are used, scaled where necessary to correspond to a train length of 400 m. It is hereby assumed that the energy from this type of EH device is dominated by the response to the

Table 7
Comparison of the energy harvested by different EH technologies on a notional high-speed railway, train speed 320 km/h, train length 400 m, 180 trains per day in each direction.

Energy source	Position (distance from track centre)	EH unit	Energy per unit, J/train	Units per km	Energy per km per day, Wh/km/day
Vibration, resonant PE (Slab track)	Rail	0.05 kg	1.6×10^{2}	10	7.9×10^{-3}
	Slab	0.05 kg	1.5×10^{3}	10	7.5×10^{-4}
	Ground, 2 m	0.05 kg	3.4×10^{4}	10	1.7×10^{-4}
Vibration, resonant PE (Ballast track)	Rail	0.05 kg	1.9×10^{2}	10	9.4×10^{-3}
	Sleeper	0.05 kg	1.2×10^{2}	10	6.3×10^{-3}
	Ground, 2 m	0.05 kg	1.4×10^{3}	10	6.9×10^{-4}
Vibration, resonant PE	Bridge	0.121 kg	1.1×10^{2}	10	5.5×10^{-3}
Vibration, non-resonant (lower train speeds, see Table 1)	Rail	PE patch	6.6×10^{5}	10	3.3×10^{-5}
	Rail	EM induction	8.2×10^{4}	10	4.1×10^{-4}
	Rail	Rack and pinion	0.69	10	0.35
	Sleeper	Ball screw MMR	20	10	10
Wind (VAWT)	1.91 m	0.25×0.25 m^2	203	10	101
	2.25 m	0.25×0.25 m^2	44	10	21.9
	2.85 m	0.25×0.25 m^2	4.9	10	2.47
	3.17 m	0.25×0.25 m^2	3.0	10	1.49
	Tunnel	0.25×0.25 m^2	145	10	72.4
Sound	5 m	per m^2	9.0×10^{5}	3000 m^2	1.4×10^{-2}
Solar (June)	Per m^2	–	–	–	627
	Discrete units	–	–	10 @ 0.25 m^2	1,570
	On noise barriers	–	–	1000 m^2	313,000
Solar (December)	Per m^2	–	–	–	175
	Discrete units	–	–	10 @ 0.25 m^2	440
	On noise barriers	–	–	1000 m^2	87,000

sequence of axle loads; thus the energy is proportional to the number of axles N_{axle} multiplied by the square of the deflection Δx, i.e. $W \propto N_{axle} \Delta x^2$, irrespective of the train speed.

These results per train pass-by are then extrapolated to estimate the total energy harvested per day, based on a notional high-speed train service of 10 trains per hour (in each direction) and 18 h' operation. Vibration-based EH units on the open route, on bridges and in tunnels are assumed to be located every 200 m for each direction, giving 10 units per route-km. The wind turbines are also assumed to be located every 200 m for each direction along the open route and in tunnels. Noise barriers are assumed to be fitted with acoustic EH devices throughout to a height of 1.5 m on both sides of the track.

For comparison, estimates of the energy that can be obtained from solar panels are also given. Data are used for London from the World Bank's 'Global Solar Atlas' [52] for a typical domestic solar panel installation of 1 kWp (for a typical efficiency of 16 % this corresponds to an area of 6.25 m^2). The average daily output is given as 3900 Wh/day in June, reducing to 1090 Wh/day in December [52]. Individual solar panels (assumed area 0.25 m^2) are considered, erected every 200 m in the open route for each direction. Alternatively, solar panels could be mounted on the top 1 m of the noise barriers on both sides of the track, but with an assumed 50 % reduction in efficiency to allow for their inclination.

Discussion

Although these comparisons are based on indicative assumptions about the number and size of EH units and the number of train passages, it can be seen that most forms of vibration-based EH can only yield very small amounts of energy. Resonant PE produces slightly less than 10 mWh/km/day when installed on the rail, and even less when installed on the slab, sleepers or ground. EM vibration-based EH has the potential to generate much more, especially when combined with MMR systems, but these are unproven for high-speed traffic where the rail deflections are much smaller and the excitation frequencies are higher. The main advantage of vibration-based EH is that the device can be collocated with the monitoring equipment without the need for long cables.

Acoustic EH produces nearly two orders of magnitude less power from 1 m^2 than resonant PE vibration-based EH does from a small unit with active mass 0.05 kg attached to the rail. Even if acoustic EH is deployed over large areas of noise barrier along the route, the energy produced is still small. Moreover, this technology has a low maturity.

Compared with vibration and sound, wind turbines installed close to the track have the potential to generate significant amounts of energy from the air movements induced by the passing trains, up to 100 Wh/km/day depending on the distance from the track. This neglects energy from ambient wind, which would increase this figure. Wind turbines installed in tunnels can generate similar amounts of energy. This is a mature technology with commercial/industrial applications, and it has significant potential for installation on railway infrastructure.

Although installing solar panels along long sections of noise barrier may not be practical, using single units with an area of 0.25 m^2 placed every 200 m (on each side) in open route could generate 0.4 ~ 1.6 kWh/km/day. This is many orders of magnitude greater than that achieved with vibration or sound EH and is 4–16 times the energy produced by an equal number of wind turbines installed close to the track. However, solar energy is seasonal and limited to daytime, whereas the wind EH can produce power continuously whenever a train passes.

There are several potential challenges for integration of EH on railway infrastructure, which are beyond the scope of the present study. EH devices must be attached to railway components (e.g., rails, sleepers, etc) without compromising their mechanical integrity. They must withstand harsh environmental conditions and maintain performance with minimal maintenance. It is also necessary to consider the electronics and power management of these systems.

Conclusions

A review and comparative analysis has been conducted on the application of energy harvesting on railway civil infrastructure, focusing on the potential and feasibility of utilizing vibration, sound, wind and solar sources of energy, particularly for high-speed railways.

A range of types and scales of vibration-based EH devices has been assessed, concentrating where possible on those for which field applications are available. The piezoelectric devices considered are small and can provide power between 1 μW and 4 mW depending on their type and location. EH devices based on electromagnetic induction can deliver significantly greater power due to their larger size. Most of the vibration-based EH devices attached to the track (or bridges) can supply sufficient power for individual low-power sensors for structural health monitoring, but their output is insufficient for higher-power applications or for data transmission unless energy storage devices are included. Vibration-based EH on the ground generates insufficient power, as does a PE patch on the rail. Harvesting energy from acoustic sources would require deployment over very large areas to deliver practical amounts of energy, and this technology is currently less mature.

For both open route and tunnels, small wind turbines close to the track and driven by passing trains have the greatest potential. These have a high technology readiness level, and depending on the location, they could harvest 3–5 orders of magnitude more energy than piezoelectric vibration-based EH.

Solar panels, considered for comparison, have the potential for even greater energy generation. For example, single panels of area 0.25 m^2 could generate 4–16 times the output of the same number of wind turbines located close to the track. Solar panels could also be installed on noise barriers allowing many more times this energy to be generated. However, their output is confined to daylight conditions and dependent on the weather.

For specific applications, more detailed analysis would be required, taking account of the likely power requirements, and considering operational parameters. More detailed study is required of the flow speeds around the train and their interaction with wind turbines close to the track. In addition, the expected durability should be assessed and whole life costs should be determined and compared with the potential benefits. The results presented here are examples based on current implementations of the different technologies; their performance is likely to improve in the future.

CRediT authorship contribution statement

Wenjing Sun: Writing – original draft, Visualization, Investigation, Formal analysis. **David J. Thompson:** Writing – original draft, Visualization, Supervision, Methodology, Investigation, Formal analysis, Conceptualization. **Daniil Yurchenko:** Writing – review & editing, Supervision, Methodology, Conceptualization. **Dong Zhao:** Writing – original draft, Investigation, Formal analysis. **Zhenhua Luo:** Writing – review & editing, Funding acquisition. **Irfan Khan:** Writing – review & editing, Project administration, Funding acquisition, Conceptualization.

Declaration of competing interest

The authors declare that they have no known competing financial interests or personal relationships that could have appeared to influence the work reported in this paper.

Acknowledgements

This study formed part of a project that was initiated and funded by HS2 Ltd through the framework of UKCRIC (UK Collaboratorium for Research on Infrastructure and Cities) which was initially funded under

EPSRC, United Kingdom, grant EP/R017727/1.

Data availability

Data will be made available on request.

References

[1] Duarte F, Ferreira A. Energy harvesting on railway tracks: state-of-the-art. Proc Institution of Civil Engineers, Transport 2017;170(TR3):123–30.
[2] Hosseinkhani A, Younesian D, Eghbali P, Moayedizadeh A, Fassih A. Sound and vibration energy harvesting for railway applications: A review on linear and nonlinear techniques. Energy Rep 2021;7:852–74.
[3] Bosso N, Magelli M, Zampieri N. Application of low-power energy harvesting solutions in the railway field: a review. Veh Syst Dyn 2021;59:841–71.
[4] Qi L, Pan H, Pan Y, Luo D, Yan J, Zhang Z. A review of vibration energy harvesting in rail transportation field. iScience 2022;25:103849.
[5] Zuo J, Dong L, Yang F, Guo Z, Wang T, Zuo L. Energy harvesting solutions for railway transportation: A comprehensive review. Renew Energy 2023;202:56–87.
[6] Yang Z, Zhou S, Zu J, Inman D. High-performance piezoelectric energy harvesters and their applications. Joule 2019;2:642–97.
[7] Wischke M, Masur M, Kröner M, Woias P. Vibration harvesting in traffic tunnels to power wireless sensor nodes. Smart Mater Struct 2011;20:085014.
[8] Gao MY, Wang P, Cao Y, Chen R, Liu C. A rail-borne piezoelectric transducer for energy harvesting of railway vibration. Journal of Vibroengineering 2016;18:4647–63.
[9] Li J, Jang S, Tang J. Implementation of a piezoelectric energy harvester in railway health monitoring. In Sensors and Smart Structures Technologies for Civil, Mechanical, and Aerospace Systems 2014, edited by J.P. Lynch, K.W. Wang, H. Sohn, Proc. of SPIE Vol. 9061, 90612Q.
[10] Cámara-Molina JC, Moliner E, Martínez-Rodrigo MD, Connolly DP, Yurchenko D, Galvín P, et al. 3D printed energy harvesters for railway bridges-Design optimisation. Mech Syst Sig Process 2023;190:110133.
[11] Shan G, Zhu M. A piezo stack energy harvester with frequency up-conversion for rail track vibration. Mech Syst Sig Process 2022;178:109268.
[12] Shan G, Wang D, Zhu M. Piezo stack energy harvesters with protection components for railway applications. Sens Actuators, A 2024;373:115454.
[13] Pourghodrat A, Nelson CA, Hansen SE, Kamarajugadda V, Platt SR. Power harvesting systems design for railroad safety. Proc IMechE Part F: J Rail Rapid Transit 2014;228(5):504–21.
[14] Cahill P, Nuallain NAN, Jackson N, Mathewson A, Karoumi R, Pakrashi V. Energy harvesting from train-induced response in bridges. J Bridg Eng 2014;19:04014034.
[15] Yuan T, Yang J, Song R, Liu X. Vibration energy harvesting system for railroad safety based on running vehicles. Smart Mater Struct 2014;23:125046.
[16] Cao Y, Zong R, Wang J, Xiang H, Tang L. Design and performance evaluation of piezoelectric tube stack energy harvesters in railway systems. J Intell Mater Syst Struct 2022. 1045389X221085654.
[17] Min Z, Sui G, Hou C, Zhang X, Shan X, Xie T. Study on energy capture characteristics of piezoelectric stack energy harvester for railway track. AIP Adv 2024;14:045311.
[18] Min Z, Du X, Zhang X, Wu W, Shan X, Xie T. Picking up railway track vibration energy using a novel doughnut-shaped piezoelectric energy harvester. Energy 2024;310:133183.
[19] Muscat A, Bhattacharya S, Zhu Y. Electromagnetic vibrational energy harvesters: a review. Sensors 2022;22(15):5555.
[20] Gao M, Li Y, Lu J, Wang Y, Wang P, Wang L. Condition monitoring of urban rail transit by local energy harvesting. Int J Distrib Sens Netw 2018;14(11).
[21] Sun Y, Wang P, Lu J, Xu J, Wang P, Xie S, et al. Rail corrugation inspection by a self-contained triple-repellent electromagnetic energy harvesting system. Appl Energy 2021;286:116512.
[22] Sun Y, Wang Y, Tian S, Huo SS, Hu M, Wu F, et al. Energy self-sufficient rail corrugation identification by a multistable piezo-electro-magnet coupled energy transducer. IEEE Trans Instrum Meas 2023;72:9004613.
[23] Hou W, Li Y, Guo W, Li J, Chen Y, Duan X. Railway vehicle induced vibration energy harvesting and saving of rail transit segmental prefabricated and assembling bridges. J Clean Prod 2018;182:946–59.
[24] Zhang X, Zhang Z, Pan H, Salman W, Yuan Y, Liu Y. A portable high-efficiency electromagnetic energy harvesting system using supercapacitors for renewable energy applications in railroads. Energ Conver Manage 2016;118:287–94.
[25] Lin T, Wang JJ, Zuo L. Efficient electromagnetic energy harvester for railroad transportation. Mechatronics 2018;53:277–86.
[26] Lin T, Pan Y, Chen S, Zuo L. Modeling and field testing of an electromagnetic energy harvester for rail tracks with anchorless mounting. Appl Energy 2018;213:219–26.
[27] Zhang T, Kong L, Zhu Z, Wu X, Li H, Zhang Z, et al. An electromagnetic vibration energy harvesting system based on series coupling input mechanism for freight railroads. Appl Energy 2024;353:122047.
[28] Pan Y, Lin T, Qian F, Liu C, Yu J, Zuo J, et al. Modeling and field-test of a compact electromagnetic energy harvester for railroad transportation. Appl Energy 2019;247:309–21.
[29] Pan Y, Zuo L, Ahmadian M. A half-wave electromagnetic energy-harvesting tie towards safe and intelligent rail transportation. Appl Energy 2022;313:118844.
[30] Ntotsios E, Thompson DJ, Hussein MFM. A comparison of ground vibration due to ballasted and slab tracks. Transp Geotech 2019;21:100256.
[31] Milne DRM, Le Pen LM, Thompson DJ, Powrie W. Properties of train load frequencies and their applications. J Sound Vib 2017;397:123–40.
[32] Fryba L. Dynamics of Railway Bridges. London: Thomas Telford; 1996.
[33] Galvín P, Romero A, Moliner E, De Roeck G, Martínez-Rodrigo MD. On the dynamic characterisation of railway bridges through experimental testing. Eng Struct 2021;226:111261.
[34] Gatti G, Brennan MJ, Tehrani MG, Thompson DJ. Harvesting energy from the vibration of a passing train using a single-degree-of-freedom oscillator. Mech Syst Sig Process 2016;66–67:785–92.
[35] Nunes-Pereira J, Costa P, Lanceros-Mendez S. Piezoelectric energy production. Chapter 3.9 in Comprehensive Energy Systems, Ibrahim Dincer (ed), Volume 3, 2018, 380-415, Elsevier, doi:10.1016/B978-0-12-809597-3.00324-2.
[36] Hussein MFM, Renno JM, Muthalif AGA. Energy harvesting from railway slab-tracks with continuous slabs. J Vib Control 2023;29:882–901.
[37] Cámara-Molina JC, Romero A, Moliner E, Connolly DP, Martínez-Rodrigo MD, Yurchenko D, et al. Design, tuning and in-field validation of energy harvesters for railway bridges. Mech Syst Sig Process 2024;208:111012.
[38] Akwa JV, Vielmo HA, Petry AP. A review on the performance of Savonius wind turbines. Renew Sustain Energy Rev 2012;16:3054–64.
[39] Mathew S, Philip GS. 2.05 - Wind turbines: evolution, basic principles, and classifications. In: Sayigh A, editor. Comprehensive Renewable Energy. Oxford: Elsevier; 2012. p. 93–111.
[40] D'Ambrosio M, Medaglia M, Vertical Axis Wind Turbines: History, Technology and Applications. Master thesis in Energy Engineering, Högskolan Halmstad, Sweden, May 2010.
[41] Pan H, Li H, Zhang T, Laghari AA, Zhang Z, Yuan Y, et al. A portable renewable wind energy harvesting system integrated S-rotor and H-rotor for self-powered applications in high-speed railway tunnels. Energ Conver Manage 2019;196:56–68.
[42] Sekhar R, Natarajan M, Chalasani C, Sukanta R, Yugandhar P. Experimental study on vertical axis wind turbine to harness wind power from rapidly moving railway locomotives. In M. Palanisamy et al. (eds.), Theoretical, Computational, and Experimental Solutions to Thermo-Fluid Systems, Lecture Notes in Mechanical Engineering, 445-50, 2021.
[43] Tairab AM, Wang X, Zhang Z, Hao D, Abdelrahman M, Salman W, et al. The Nexus of IoT technology: A renewable multi-module energy harvester for self-powered on railway. Sustain Mater Technol 2023;38:e00752.
[44] Sterling M, Baker CJ, Jordan SC, Johnson T. A study of the slipstreams of high-speed passenger trains and freight trains. Proc IMechE Part F: J Rail Rapid Transit 2008;222:177–93.
[45] Baker C, Johnson T, Flynn D, Hemida H, Quinn A, Soper D, et al. Train Aerodynamics: Fundamentals and Applications. Oxford: Butterworth-Heinemann; 2019.
[46] Brusca S, Lanzafame R, Messina M. Design of a vertical-axis wind turbine: how the aspect ratio affects the turbine's performance. Int J Energy Environ Eng 2014;5:333–40.
[47] Wang Y, Zhu X, Zhang T, Bano S, Pan H, Qi L, et al. A renewable low-frequency acoustic energy harvesting noise barrier for high-speed railways using a Helmholtz resonator and a PVDF film. Appl Energy 2018;230:52–61.
[48] Noh HM. Acoustic energy harvesting using piezoelectric generator for railway environmental noise. Adv Mech Eng 2018;10(7):1–9. https://doi.org/10.1177/1687814018785058.
[49] Thompson D. Railway Noise and Vibration: Mechanisms, Modelling and Means of Control. 2nd ed. London: Elsevier; 2024.
[50] Fahy F, Thompson D. Fundamentals of Sound and Vibration. second edition. Boca Raton FL: CRC Press; 2015.
[51] Koohi-Fayegh S, Rosen MA. A review of energy storage types, applications and recent developments. J Storage Mater 2020;27:101047.
[52] https://globalsolaratlas.info/, Global solar atlas, World Bank Group. Accessed 18/12/2024.



https://dspace.org/

Energy harvesting technologies on high-speed railway infrastructure: review and comparative analysis of the potential and practicality

Sun, Wenjing; Thompson, David J.; Yurchenko, Daniil; Zhao, Dong; Luo, Zhenhua ...

2025-02-01
Elsevier
https://doi.org/10.1016/j.seta.2025.104187
Sun W, Thompson DJ, Yurchenko D, et al., (2025) Energy harvesting technologies on high-speed railway infrastructure: review and comparative analysis of the potential and practicality. Sustainable Energy Technologies and Assessments, Volume 74, February 2025, Article number 104187

Downloaded from a DSpace repository. https://dspace.org/